



Time-resolved photoluminescence studies of the energy transfer from excitons confined in Si nanocrystals to oxygen molecules

Fujii, Minoru ; Kovalev, Dmitri ; Goller, Bernhard ; Minobe, Shingo ; Hayashi, Shinji ; Timoshenko, Victor Yu.

(Citation)

Physical Review B, 72(16):165321-165321

(Issue Date)

2005-10

(Resource Type)

journal article

(Version)

Version of Record

(URL)

<https://hdl.handle.net/20.500.14094/90000283>



Time-resolved photoluminescence studies of the energy transfer from excitons confined in Si nanocrystals to oxygen molecules

Minoru Fujii

Department of Electrical and Electronics Engineering, Faculty of Engineering, Kobe University, Rokkodai, Nada, Kobe 657-8501, Japan

Dmitri Kovalev and Bernhard Goller

Physik-Department E16, Technische Universität München, D-85747 Garching, Germany

Shingo Minobe and Shinji Hayashi

Department of Electrical and Electronics Engineering, Faculty of Engineering, Kobe University, Rokkodai, Nada, Kobe 657-8501, Japan

Victor Yu. Timoshenko

Faculty of Physics, Moscow State M. V. Lomonosov University, 119992 Moscow, Russia

(Received 11 March 2005; revised manuscript received 4 August 2005; published 17 October 2005)

The formation of singlet oxygen due to the energy transfer from excitons confined in silicon nanocrystals to oxygen molecules is studied using time-resolved photoluminescence spectroscopy. The process of the excitation of oxygen molecules from the ground triplet state to the second excited singlet state is studied at low temperatures, where oxygen molecules are physisorbed on the surface of silicon nanocrystals and at room temperature in gaseous oxygen ambient and in oxygen-saturated water. The low temperature measurements reveal that the energy transfer time is the shortest for the resonant energy transfer. The involvement of one energy-conserving transversal optical phonon results in about 40% increase of the energy transfer time. The excitation rate of oxygen dimers is found to be similar to that measured for oxygen molecules. At room temperature, the time of the energy transfer to oxygen molecules is about 17 μ s. The photosensitizing efficiency of silicon nanocrystals at room temperature is found to be as high as 80% for gaseous oxygen ambient and for oxygen-saturated water.

DOI: [10.1103/PhysRevB.72.165321](https://doi.org/10.1103/PhysRevB.72.165321)

PACS number(s): 78.30.Ly, 78.35.+c, 78.45.+h, 68.03.Fg

I. INTRODUCTION

Bulk silicon (Si) is, due to its indirect band-gap electronic structure, a very inefficient light emitter. In recent years several technological approaches have been developed towards improving the efficiency of light emission from nanosilicon-based structures. Si nanocrystal assemblies can be prepared in different ways. The most widely discussed system is known as porous silicon (PSi).¹ Structural investigations have confirmed that it consists of Si nanocrystals of different sizes (typically a few nm) and shapes. PSi can be fabricated by electrochemical anodization of Si wafers in hydrofluoric acid-based solutions.¹ It has attracted most of interest due to the simplicity of the preparation procedure and the high emission efficiency under optical excitation (up to 10%). Other examples are Si nanocrystal assemblies prepared via ion implantation into a SiO₂ matrix,² by reactive Si deposition onto fused quartz,³ by plasma enhanced chemical vapor deposition,⁴ by magnetron sputtering,⁵ by an aerosol procedure,⁶ or by laser pyrolysis of Silane.⁷ Detailed spectroscopic studies demonstrated that all these systems show strong near infrared and visible photoluminescence (PL) with characteristics very similar to those of PSi.

It was soon realized that, despite the high PL quantum yield achieved, a long lifetime of excitons confined in Si nanocrystals is an inherent limitation for light emitting appli-

cations of Si nanocrystal assemblies.¹ However, this is certainly an advantage for other possible applications since electronic excitation (exciton) energy is stored over a time scale of 10⁻⁴ s and, if required conditions are fulfilled, this energy can be efficiently transferred to other substances, i.e., silicon nanocrystals can be efficient energy donors. As an example, recently we found a type of singlet molecular oxygen generator based on silicon nanocrystal assemblies.⁸⁻¹⁰ Singlet oxygen (¹O₂) (Ref. 11-13) is an electronically excited state of oxygen molecules (O₂) and is a very important substance in biology and chemistry because it mediates important processes in organic molecules.^{12,14} One of the most important applications of singlet oxygen is a photodynamic therapy of cancer.¹⁵ Thus the capability of Si nanocrystal assemblies to generate ¹O₂ is an interesting prospect for applications of the most commonly used semiconductor in chemistry, biology, and medicine.

From detailed spectroscopic studies of porous silicon whose surface at low temperatures was covered by physisorbed O₂ it has been concluded that the whole effect is based on the energy transfer from excitons confined in Si nanocrystals to O₂ via the exchange of single electrons having opposite spins which results in spin-flip activation of O₂.⁸ During this process electrons are exchanged between triplet excited states of energy donors, i.e., photoexcited Si nanocrystals, and triplet ground states of energy-accepting

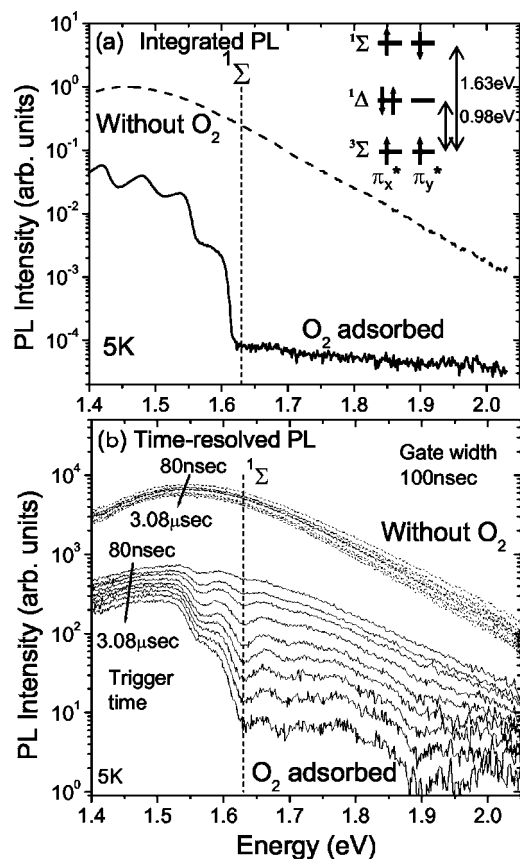


FIG. 1. (a) CW PL spectra of a *PSi* layer in vacuum (dashed line) and a layer having physisorbed oxygen molecules on the surface (solid line) at 5 K. Electron-spin configurations and spectroscopic labeling of molecular oxygen states are shown in the inset. (b) Time-resolved PL spectra at 5 K (dashed line, in vacuum; solid line, with physisorbed oxygen molecules). The measurement gate width is 100 ns. The data for the measurement delay time with respect to the excitation pulse of 0.08, 0.18, 0.28, 0.48, 0.78, 1.08, 1.48, 2.08, 3.08 μ s are shown.

O_2 .⁹ It has been demonstrated that O_2 are excited to either a first-excited $^1\Delta$ state (0.98 eV from the ground $^3\Sigma$ state) or a second-excited $^1\Sigma$ state (1.63 eV from the ground $^3\Sigma$ state) depending on the band-gap energies of Si nanocrystals participating in the energy transfer [see inset of Fig. 1(a)]. During the energy transfer forming the $^1\Sigma$ state, orbital angular momentum conservation is fulfilled, while for the $^1\Delta$ state, a change of angular momentum of O_2 ($\Delta L=2$) is required. This restriction results in relatively weak coupling between excitons and O_2 forming the $^1\Delta$ state, while their interaction followed by generation of the $^1\Sigma$ state is very efficient.

For O_2 -physisorbed *PSi*, the strong coupling to the $^1\Sigma$ state results in an almost complete suppression of exciton photoluminescence (PL) band above the energy of the $^1\Sigma$ state. On the other hand, only partial PL quenching occurs below the energy of the $^1\Sigma$ state, since in this energy range coupling can form only the $^1\Delta$ state.⁹ By analyzing partially quenched PL spectra, the mechanism of the energy transfer following the $^1\Delta$ state has been studied in detail.⁹

One of the purposes of this work is the investigation of the energy transfer process forming the $^1\Sigma$ state of O_2 using

time-dependent analysis of the energy transfer-related PL features at low temperatures (Sec. III A). At liquid He temperature, the lifetime of the ground triplet state of excitons confined in silicon nanocrystals is in the millisecond range^{1,16} and the number of O_2 physisorbed on the surface of Si nanocrystals is large. As a result, both singlet states of O_2 can be excited efficiently. At room temperature, the lifetime of excitons is controlled by a shorter lifetime of the singlet excited exciton states and the energy transfer can proceed only during short collisions of O_2 with the surface of Si nanocrystals. In an energy transfer process the time of energy transfer to an acceptor always competes with the lifetime of electronic excitations of an energy donor. Since at room temperature the rate of the energy transfer forming the $^1\Delta$ state is smaller than the exciton radiative recombination rate, only the excitation of the $^1\Sigma$ state is efficient.⁹

In Secs. III B and III C, we report on room temperature time-resolved spectroscopic studies of the energy transfer from excitons confined in Si nanocrystals to O_2 in gaseous oxygen ambient and in oxygen-saturated water, respectively. We demonstrate that the time of the energy transfer is shorter than the exciton lifetime. This results in a high efficiency of the energy transfer, exceeding 85% for oxygen ambient and 75% for oxygen-saturated water.

II. EXPERIMENTAL DETAILS

Porous Si layers were prepared by standard electrochemical etching¹⁷ of (100) oriented, boron-doped bulk Si substrates with a typical resistivity of 5–15 Ω cm in a 1:1 by volume mixture of hydrofluoric acid (50 wt. % in water) and ethanol. The current density was 50 mA/cm². For low temperature PL measurements, thin layers of *PSi* were mounted on a cold finger of a cryostat. The cryostat was first evacuated to 5×10^{-6} torr, then filled by O_2 gas to 7 torr at 150 K, and finally cooled down to 5 K to physisorb O_2 on the surface of Si nanocrystals. For room temperature PL measurements, free-standing *PSi* layers were detached from Si substrates via an electropolishing step,¹ immersed in CCl_4 , and transferred to *PSi* powder in an ultrasonic bath. A quartz cuvette containing nanostructured powder was mounted in an optical cryostat and experiments were performed either in vacuum or with a given pressure of O_2 ambient in the sample chamber. *PSi* powder was also immersed into either degassed or O_2 -saturated water. During optical measurements the solution was permanently mixed using a magnetic stirrer.

For continuous wave (CW) PL measurements, an Ar⁺ ion laser (excitation energy 2.41 eV) with the excitation power of less than 10 mW/cm² was used. PL spectra were recorded using a spectrometer equipped with a Si charge-coupled device (CCD). For time-resolved PL measurements, the excitation source for low temperature experiments was an optical parametric oscillator pumped by a pulsed Nd:YAG laser (excitation energy: 2.58 eV, pulse energy density: 2.5 mJ/cm², repetition frequency: 20 Hz, pulse duration: 5 ns), and for room temperature experiments, a frequency-doubled Nd:YAG laser (excitation energy: 2.33 eV, pulse energy: 1 mJ, repetition rate: 10 Hz, pulse duration: 8 ns). Spectrally and time-resolved intensity of the emitted light

was measured using a monochromator equipped with a photomultiplier or a gated CCD (PI-Max, Princeton Instrument, detection energy: 1.3–2.5 eV, 5 ns response time) triggered by exciting laser pulse. PL detection delay time with respect to the excitation pulse and measurement gate time were varied simultaneously. As references, time-resolved PL spectra of the same samples were always taken in oxygen-free ambient. All spectra were corrected on the spectral sensitivity of the optical systems.

III. RESULTS AND DISCUSSION

A. Energy transfer from excitons to oxygen molecules at low temperatures

First of all, we demonstrate the difference in the efficiency of energy transfer from excitons to different singlet excited states ($^1\Delta$ and $^1\Sigma$) of O_2 in Fig. 1(a). A broad and featureless PL band of *PSi* measured in vacuum under CW optical excitation (dashed line) reflects residual size and shape distribution of Si nanocrystals assembling *PSi* layers. When O_2 is physisorbed on the surface of Si nanocrystals the periodic spectral features appear [solid line in Fig. 1(a)]. They arise from the emission of multiple phonons required to conserve energy during the energy transfer from excitons to O_2 followed by the excitation of the $^1\Delta$ state.^{8,9} Emission of Si nanocrystals above the $^1\Sigma$ state energy is completely quenched due to extremely efficient energy transfer followed by the excitation of the $^1\Sigma$ state and spectroscopic investigation of the energy transfer mechanism is not possible.

Figure 1(b) shows time-resolved PL spectra of a *PSi* layer in vacuum and that containing physisorbed O_2 at the surface of Si nanocrystals. The gate width is kept constant (100 ns) while the delay time with respect to the excitation pulse is varied from 80 ns to 3.08 μ s. In vacuum, the PL spectral shape and its intensity do not change significantly within the time scale investigated. The very long PL lifetime at low temperatures is caused by the population of excitons in optically inactive triplet states.^{16,18,19} On the other hand, under presence of O_2 , already at 80 ns delay time with respect to PL excitation pulse, PL features can be distinguished and a very strong variation of the PL spectral shape appears as the delay time of the PL measurements is increased (note the semilogarithmic scale of Fig. 1). The spectra shown in Fig. 1(b), apparently, can be divided into two spectral ranges. In the low energy range (below ~ 1.55 eV) the PL lifetime is relatively long and no distinct PL features are observed. In the high energy range the PL lifetime is much shorter and a number of PL signatures related to the energy transfer process can be clearly distinguished.

The exact shape of time-resolved PL spectra of a *PSi* layer containing physisorbed O_2 is a product of the size distribution, the spectral dependence of the recombination rates of excitons in vacuum [$\tau_0(\omega)^{-1}$], and that of the energy transfer rate [$\tau_{ET}(\omega)^{-1}$]. In a simplified model, the time transient of the PL intensity of *PSi* containing physisorbed O_2 and *PSi* in vacuum can be expressed as $I_{Oxygen}(\omega, t) = I_0(\omega) \exp[-(\tau_0(\omega)^{-1} + \tau_{ET}(\omega)^{-1})t]$ and $I_{vac}(\omega, t) = I_0(\omega) \times \exp[-\tau_0(\omega)^{-1}t]$, respectively. Here $I_0(\omega)$ accounts for the

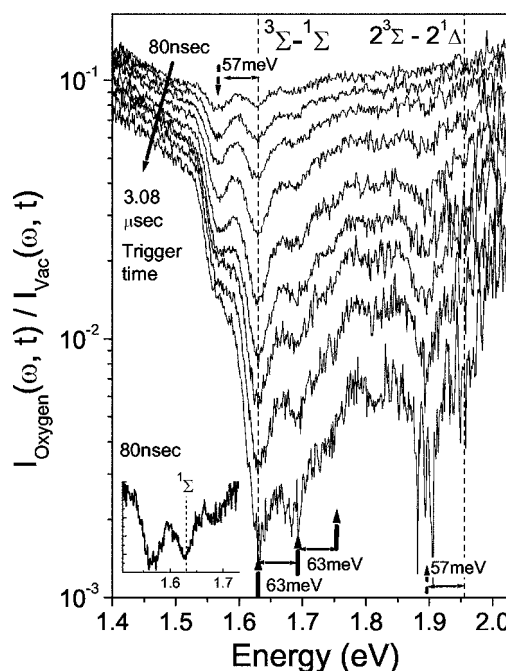


FIG. 2. Time-resolved PL spectra of a *PSi* layer having oxygen molecules physisorbed on the surface divided by those of *PSi* in vacuum [$I_{Oxygen}(\omega, t)/I_{vac}(\omega, t)$]. The measurement gate width is 100 ns. The data for the measurement delay time with respect to the excitation pulse of 0.08, 0.18, 0.28, 0.48, 0.78, 1.08, 1.48, 2.08, 3.08 μ s are shown. The energy positions of the $^3\Sigma - ^1\Sigma$ transition of O_2 and that of the $2^3\Sigma - 2^1\Delta$ transition of oxygen dimers are indicated by dashed lines.

PL envelope function caused by the size distribution. By dividing $I_{Oxygen}(\omega, t)$ by $I_{vac}(\omega, t)$ measured at the same measurement gate duration and delay time, the spectral dependence of the “energy transfer intensity” is obtained, and from its temporal behavior, the energy transfer rate can be estimated.

Figure 2 shows the results of this division [$I_{Oxygen}(\omega, t)/I_{vac}(\omega, t)$]. It should be noted that at 80 ns delay time, $I_{Oxygen}(\omega, t)/I_{vac}(\omega, t)$ is about 0.1. This implies that a very fast nonradiative recombination process is additionally introduced by adsorbed O_2 . A large fraction of Si nanocrystals do not contribute to the emission. The fact that the quenching at 80 ns delay time occurs almost uniformly in the entire spectral range, even at very low energy, where excitons can couple only to the $^1\Delta$ state, indicates that the PL quenching is not related to the energy transfer. Another process which is known to be responsible for *PSi* PL quenching in the presence of adsorbed O_2 is charge transfer. It has been demonstrated that optically charged Si nanocrystals²⁰ or *p*- or *n*-doped ones do not contribute to the PL due to very efficient Auger nonradiative process.²¹ Adsorption of NO_2 molecules on the surface of Si nanocrystals results also in a very efficient structureless PL quenching. NO_2 molecules are very efficient electron acceptors and the hole remaining in Si nanocrystals quenches completely the PL.²² O_2 molecule is known to be a very efficient electron acceptor as well and, therefore, Auger PL quenching can efficiently compete with the mechanism of the energy transfer. Since we are interested

in the energy transfer to O_2 , we will mainly concentrate on the spectral dependence measured at longer delay time.

In Fig. 2, already at the delay time of 80 ns two distinct minima can be seen at around 1.6 eV. The expansion of this spectral range is shown in the inset (lower left part of Fig. 2). These minima appear at exactly the energy of the $^1\Sigma$ state (1.63 eV) and about 57 meV below. The low energy minimum corresponds to a partially quenched step observed in CW PL spectra [Fig. 1(a)]. This step was explained in Ref. 9 as follows. In bulk Si, the bottom of conduction band is located in the vicinity of the X points of the Brillouin zone (Δ minima), and therefore emission or absorption of momentum-conserving phonons are required for the optical transition. The transversal optical [TO(Δ)] phonon-assisted transition is the dominant for bulk Si and the exciton emission line appears 57 meV (TO phonon energy at Δ minima) below the free exciton transition.²³ For Si nanocrystals similarly, the TO(Δ) phonon-assisted transition is reported to be the dominant recombination path even for very small nanocrystals.^{16,18,19,24} If Si nanocrystals have the band-gap energy at 1.63 eV, they can transfer energy resonantly to O_2 . Since, without O_2 physisorption, these nanocrystals luminesce at 1.57 eV due to emission of one TO(Δ) phonon, an additional PL quenching appears at around 1.57 eV.

If Si nanocrystals had a strictly indirect band-gap nature, only one minimum should appear at around 57 meV below the $^1\Sigma$ energy. However, a minimum exists also exactly at the energy of the $^1\Sigma$ state, implying that the probability of a quasidirect no-phonon optical transitions is not small and it can compete with the TO(Δ) phonon-assisted transition. The quasidirect transitions become partially allowed in Si nanocrystals due to the uncertainty in the momentum space for carriers caused by their spatial confinement in a space smaller than the exciton Bohr radius of bulk Si.

We would like to note that in Fig. 2 at the delay time of 80 ns, the minimum at 57 meV below the $^1\Sigma$ energy is even deeper than the minimum at the resonant energy. This suggests that the TO(Δ) phonon-assisted recombination is a dominant recombination path even for relatively small nanocrystals having a band-gap energy of 1.63 eV. This conclusion is consistent with that obtained from resonant PL spectroscopy.²⁴

In Fig. 2, the minimum at 1.63 eV grows as the delay time is increased, while that at 1.57 eV saturates. Because of nearly equal probability of direct and indirect recombination paths for nanocrystals having the band-gap energy in this range, two groups of Si nanocrystals always contribute to the PL at the same energy. For example, the PL at 1.57 eV consists of that due to direct exciton recombination of nanocrystals having the band gap at 1.57 eV and TO(Δ) phonon-assisted recombination of those having the band gap at 1.63 eV (1.57 eV + 57 meV) (see Fig. 3). The second group can contribute to the energy transfer followed by the excitation of the $^1\Sigma$ state, while the first one cannot. They couple to O_2 very weakly and thus their PL intensity is almost not changed because the time scale of the energy transfer forming the $^1\Delta$ state is several hundreds of microseconds.⁹ On the other hand, groups of nanocrystals contributing to the PL at 1.63 eV have band gaps equal to or larger than the $^1\Sigma$ state

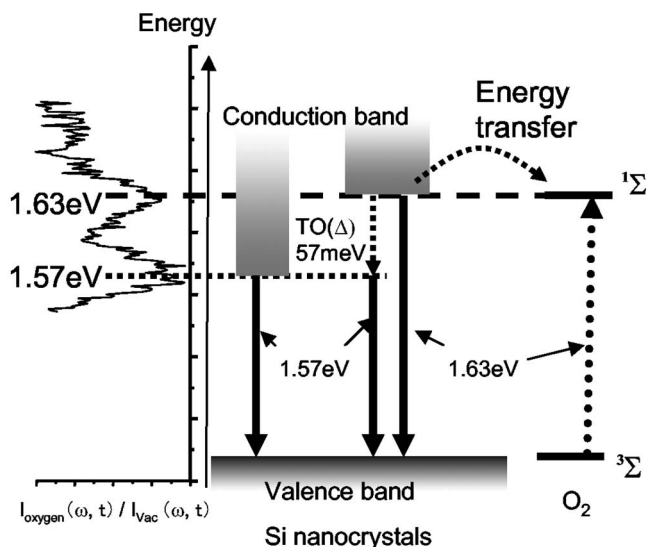


FIG. 3. Sketch of energy-level diagram of molecular oxygen and Si nanocrystals having the band-gap energies of 1.63 eV and 1.57 eV. Both nanocrystals luminesce at 1.57 eV, while only the first one can contribute to the energy transfer followed by the $^1\Sigma$ state excitation. $I_{\text{oxygen}}(\omega, t)/I_{\text{vac}}(\omega, t)$ at 80 ns delay time is shown on the left side.

energy and thus can transfer energy quickly, resulting in the absence of saturation of the energy transfer efficiency.

For nanocrystals having a band-gap energy larger than 1.63 eV, an excess of the excitation energy with respect to the $^1\Sigma$ state energy has to be released by the emission of energy-conserving phonons. This process is most probable for phonons having the highest density of states which in bulk Si are transverse optical phonons being almost at the center of the Brillouin zone [TO(Γ)] with an energy of 63 meV. If the band-gap energy of Si nanocrystals does not coincide with the $^1\Sigma$ state energy plus an integer number times the TO(Γ) phonon energy, the additional emission of acoustic phonons is required to conserve the energy. This process has a smaller probability and the rate of energy exchange is reduced. Consequently, quenching maxima appear with the period of 63 meV above the energy of the $^1\Sigma$ state. In Fig. 2, the periodic features are indicated by solid arrows. We can see that the energy transfer time becomes longer and the features become less resolved with an increase of the number of energy-conserving phonons.

In Figs. 1(b) and 2, additionally to features corresponding to the energy transfer to the $^1\Sigma$ state of O_2 , a quenching band appears in the range between 1.86 and 1.97 eV. This band is apparently not related to the energy transfer resulting in the generation of the $^1\Sigma$ state. From the energy position of the band, it can be attributed to the excitation of O_2 dimers [$(O_2)_2$, pairs of neighboring O_2 molecules], i.e., the electronic transition from $2^3\Sigma-2^1\Delta$ states of $(O_2)_2$ (~ 1.96 eV).²⁵

Figure 2 clearly demonstrates that the rate of the energy transfer to $(O_2)_2$ is much higher than that of the $^3\Sigma-^1\Delta$ transition and is similar to the rate of the $^3\Sigma-^1\Sigma$ transition. The high efficiency of the $2^3\Sigma-2^1\Delta$ transition of $(O_2)_2$ compared to the $^3\Sigma-^1\Delta$ transition of an oxygen molecule is

caused by a spin-conserving electron exchange among the two $^3\Sigma$ states.⁹ In this process, excitons provide only the energy to activate the process of exchange of electrons having opposite spins between a pair of oxygen molecules. Therefore spin configuration of excitons with respect to spins of O_2 is not crucial. From the point of view of practical applications, direct excitation of oxygen dimers implies the creation of two 1O_2 by one exciton (and by one photon), and thus is an efficient 1O_2 generation path.

It is interesting to note that the high-energy band includes two PL quenching minima (see Fig. 2). The higher-energy minimum is exactly at the $2^3\Sigma-2^1\Delta$ transition energy (1.96 eV),²⁵ while the lower-energy one is about 57 meV below. These two minima can be more clearly distinguished in Fig. 1(b). The origin of the lower-energy minimum can be explained by the same model described above, i.e., Si nanocrystals having a band-gap energy of 1.96 eV exhibit PL at 1.90 eV due to the emission of one momentum-conserving TO(Δ) phonon and thus PL quenching caused by the energy transfer to oxygen dimers appears at around 1.90 eV. This result again implies that the indirect band-gap nature of bulk Si is still strongly held for very small Si nanocrystals with the band-gap energy of 1.96 eV. In principle, we can roughly estimate the ratio of indirect to quasidirect recombination paths from the depth of the two minima in Fig. 2. Although quantitative estimation is not possible due to the strong background signal arising from the energy transfer to the $^1\Sigma$ state of O_2 monomers, the present result seems to suggest that indirect recombination of excitons is still dominant in very small Si nanocrystals having a band-gap energy of 1.96 eV.

The spectral dependence of the energy transfer time can quantitatively be discussed if we convert Fig. 2 into time dependence of $I_{Oxygen}(\omega, t)/I_{Vac}(\omega, t)$. Figure 4 shows the result. To neglect the very fast component, $I_{Oxygen}(\omega, t)/I_{Vac}(\omega, t)$ is normalized to 1 at 80 ns delay time. The slope corresponds to energy transfer time. We can see that energy transfer time is the shortest at 1.63 eV, and is about 320 ns. The energy transfer time becomes longer with an increasing number of TO(Γ) energy-conserving phonons emitted during the energy exchange. It is about 450 ns when one TO(Γ) phonon is involved in the process (1.69 eV). $I_{Oxygen}(\omega, t)/I_{Vac}(\omega, t)$ at 1.57 eV decreases very fast at the initial stage and then starts to saturate. This behavior can be clearly seen in Fig. 4 (dashed curve). The slope finally approaches that measured at 1.44 eV, where excitons can couple only to the $^1\Delta$ state. We note that the estimated energy transfer time is not necessarily that of a single O_2 , but all O_2 adsorbed on the surface of a nanocrystal can be treated as a single quenching system. The energy transfer rate to a single O_2 can be obtained by dividing the decay rate by the number of O_2 adsorbed on a single nanocrystal. In a previous work,⁹ we roughly estimated the number of adsorbed O_2 per nanocrystal from partially quenched PL spectra of Si nanocrystals at nearly the same condition as in the present work. The estimated value was 8. If we take this value, the time of the resonant energy transfer from exciton confined in a Si nanocrystal to a single oxygen molecule is about 2.56 μ s.

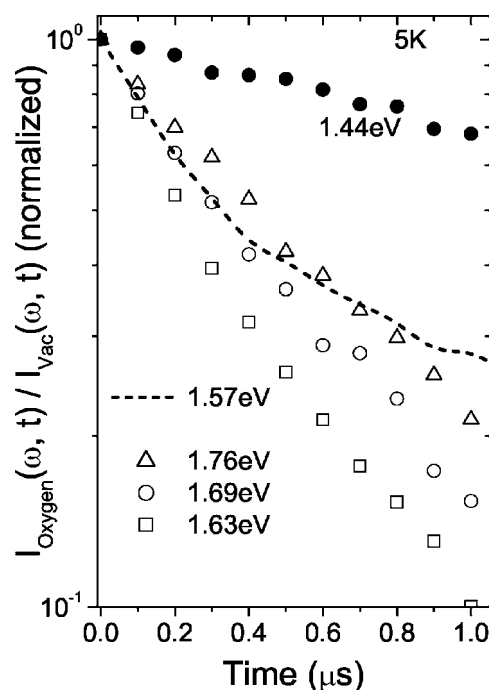


FIG. 4. $I_{Oxygen}(\omega, t)/I_{Vac}(\omega, t)$ as a function of time at detection energies of 1.44, 1.57, 1.63, 1.69, and 1.76 eV. The energy transfer time can be estimated from the slopes.

B. Energy transfer from excitons to oxygen molecules in gaseous phase

To demonstrate the efficient energy transfer from Si nanocrystals to O_2 at room temperature we measured PL spectra of H-terminated PSi in vacuum (Fig. 5, dotted line) and at 1 bar of O_2 ambient (Fig. 5, solid line). The presence of oxygen ambient results in a strong reduction of the PL intensity. The suppression level depends on the detection energy. To eliminate the influence of the size distribution on the shape

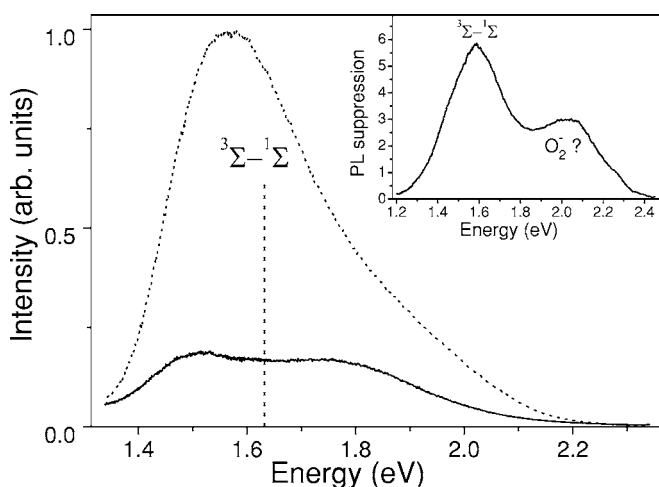


FIG. 5. PL spectra measured in vacuum (dotted line) and in oxygen ambient at 1 bar (solid line). Inset: spectral dependence of the PL suppression level measured at 1 bar of O_2 ambient. $T = 300$ K, $E_{ex} = 2.54$ eV. Energy of the $^3\Sigma-^1\Sigma$ transition of O_2 is indicated by a dotted line.

of the quenched PL spectra we again define the PL suppression level as the ratio of the PL intensity measured in vacuum to that measured in O_2 ambient. As mentioned above, the spectral dependence of the PL suppression level represents the energy-dependent coupling strength of excitons and O_2 (inset of Fig. 5). The PL suppression level is maximal at ~ 1.63 eV. The spectral feature related to the energy transfer is significantly broadened since energies of excitons and oxygen molecules are not well defined at high temperatures. The absence of spectral features at lower energies due to possible $^3\Sigma \rightarrow ^1\Delta$ transitions of O_2 indicates that, contrary to low temperatures, only the $^3\Sigma \rightarrow ^1\Sigma$ transition is involved in the energy transfer process. The suppression of the PL intensity at room temperature is almost equal to 6. From the spectral behavior of the PL quenching level it follows that if an exciton does not contribute to the light emission it necessarily activates a singlet O_2 state. This implies that more than 80% of the photoexcited excitons transfer their energies to O_2 and the efficiency of singlet oxygen generation exceeds 0.8. This allows us to estimate the generation rate of singlet O_2 in the pores of *PSi*. For ambient O_2 pressure and a 1 W/cm^2 illumination intensity this value is $\sim 5 \times 10^{20}$ singlet oxygen molecules/ $\text{cm}^3 \text{ s}$.

We would like to mention that there is additionally another weaker local maximum in the spectral dependence of the PL suppression level around 2 eV. One of the possible reasons for that is the formation of the superoxide (O_2^-) state mediated by excitons. O_2 is a very good acceptor and electrons can be donated by photoexcited excitons. In this scenario nanocrystals become positively charged and cannot contribute to the PL due to highly efficient Auger process.²⁶

The strong PL suppression in oxygen ambient indicates that the energy transfer process competes efficiently with the radiative recombination channel even at room temperature. Since rates of both processes are energy dependent, we again performed time-resolved PL studies in order to resolve details of the energy exchange process. Time-resolved PL spectra measured in vacuum demonstrate a continuous spectral shift towards lower energies with the increase of the delay time of the PL detection with respect to the excitation pulse [see Fig. 6(a)]. This is a direct consequence of quantum confinement: for larger nanocrystals optical transition oscillator strength is smaller and exciton lifetime is longer. Therefore, they persist and contribute to the PL longer. In the presence of oxygen ambient [Fig. 6(b)] no noticeable difference from PL measured in vacuum is seen for the delay time up to 10 μs and, obviously, the energy transfer process requires longer time. A clear difference can be detected at the delay time equal to 20 μs . In the presence of oxygen ambient, a local minimum around 1.6 eV appears in the PL spectrum. This supports the observation made at low temperatures that excitons having energies in the vicinity of 1.63 eV (energy of the $^3\Sigma - ^1\Sigma$ transition) do not contribute to the PL due to efficient energy transfer to oxygen molecules. With an increase of the delay time, the high energy side of the PL band is suppressed further while the PL below 1.5 eV is almost not affected. Excitons having energies above 1.63 eV also transfer their energies to O_2 but the process is less efficient. For excitons having energies smaller than the energy of the $^3\Sigma - ^1\Sigma$ transition of O_2 the energy transfer, contrary to cryo-

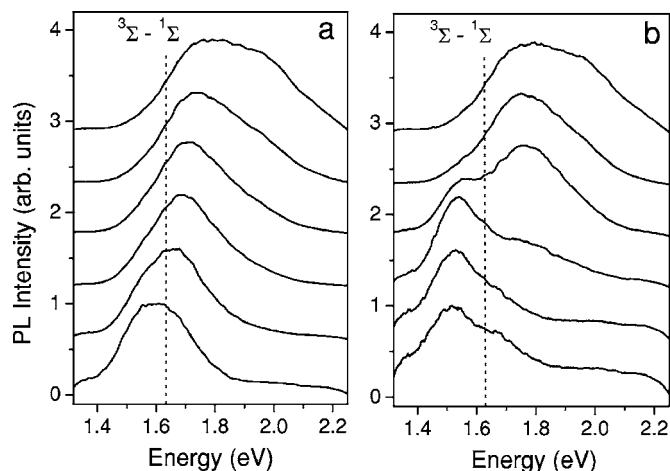


FIG. 6. Time-resolved PL spectra of *PSi* in vacuum (a) and in oxygen ambient at 1 bar (b). Different delay times of PL measurements with respect to the excitation pulse and measurement gate times have been used. From the top to the bottom: delay time 0, 10, 50, 100, 250, 500 μs , gate time 1, 10, 20, 50, 100, 1000 μs , respectively. $E_{ex} = 2.33$ eV. Energy of the $^3\Sigma - ^1\Sigma$ transition of O_2 is indicated by a dotted line. All PL spectra are normalized to 1.

genic temperatures,⁹ is still possible due to thermal broadening effects. This can be seen as a PL suppression up to 100 meV below 1.63 eV (~ 4 kT). At lower energies no significant PL reduction with respect to the measurements performed in vacuum can be detected. At cryogenic temperatures the energy transfer to the $^1\Delta$ state of O_2 has been observed since exciton lifetime exceeds a millisecond¹ while the time of the energy transfer was found to be $\sim 300 \mu\text{s}$. Contrary to cryogenic temperatures at room temperature the energy transfer to the $^1\Delta$ state of O_2 is very inefficient because it cannot compete with the exciton decay rate.

In the presence of oxygen ambient an exciton can either annihilate radiatively or nonradiatively via energy transfer to oxygen molecules, and the exciton recombination rate measured in oxygen ambient $\tau_{meas}(\omega)^{-1}$ is a sum of that in vacuum $\tau_0(\omega)^{-1}$ and the energy transfer rate $\tau_{ET}(\omega)^{-1}$. To find the spectral dependence of the energy transfer time $[\tau_{ET}(\omega)]$ we measured separately the exciton lifetimes in vacuum and in oxygen ambient (Fig. 7). The exciton lifetimes measured in vacuum exhibit strong spectral dispersion due to quantum confinement effects.^{1,16} The presence of oxygen ambient results in a strong reduction of the exciton lifetime over the complete spectral range investigated. This, however, does not imply that the energy transfer time is similar for excitons having different energies. In the inset of Fig. 7 we plot the spectral dependence of the energy transfer time recalculated on the basis of measured $\tau_0(\omega)$ and $\tau_{meas}(\omega)$. Again, the energy transfer time is the shortest for excitons whose energies coincide with the energy of the $^3\Sigma - ^1\Sigma$ transition of O_2 and is about 17 μs at 1 bar of O_2 ambient. For higher energies the exciton lifetimes are slightly longer and for lower energies they are significantly longer. For higher energies the energy transfer is accompanied by the emission and for lower energies by the absorption of phonons whereas their emission is always more probable than their absorption.

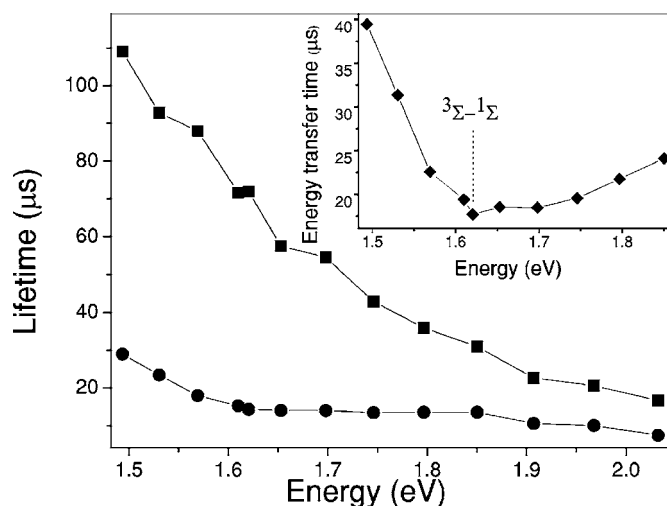


FIG. 7. Spectral dependencies of the PL lifetime measured in vacuum (squares) and at 1 bar of oxygen ambient (circles). Inset: spectral dependence of the energy transfer time in oxygen ambient at 1 bar. $T=300$ K, $E_{ex}=2.33$ eV. Energy of the $^3\Sigma-^1\Sigma$ transition of O_2 is indicated by a dotted line.

Despite a relatively long energy transfer time it is still significantly shorter than the lifetime of indirect excitons confined in Si nanocrystals, which explains the high efficiency of the energy transfer process (see Fig. 5). Therefore, the difference in the efficiency of the energy transfer between cryogenic and room temperatures is mainly governed by the difference in the number of oxygen molecules at the surface of Si nanocrystals and not by the difference in the exciton lifetime.¹

C. Energy transfer from excitons to oxygen molecules in water

For biological and medical applications of singlet oxygen, its generation in oxygen-containing aqueous solutions is crucial. Unfortunately, fast nonradiative vibrational relaxation processes of 1O_2 in water ($3.1 \mu s$) (Ref. 13) makes the detection of PL from 1O_2 dissolved in water extremely difficult. However, even if the emission line due to the radiative $^1\Delta-^3\Sigma$ transition of 1O_2 is not detected, the energy transfer can be indirectly probed by monitoring the shape of the PL band and the lifetimes of excitons in the presence of dissolved O_2 . In Fig. 8 we demonstrate PL spectra from *PSi* powder immersed in oxygen-saturated water (solid line) and in water after a degassing procedure (dotted line). O_2 dissolved in water causes a similar PL quenching effect as in gaseous oxygen ambient. To obtain the spectral dependence of the energy transfer efficiency for oxygen-saturated water we use the procedure identical to that employed for gaseous O_2 ambient. Although the PL suppression level is weaker, its spectral shape is almost identical to that measured in gaseous O_2 . This evidences the formation of singlet oxygen in water and indicates that the energy exchange mechanism should be similar. From the PL suppression level it follows that the efficiency of the energy transfer in oxygen-saturated water is equal to 75%.

Finally we determined the energy transfer time for oxygen-saturated water following the same procedure as for

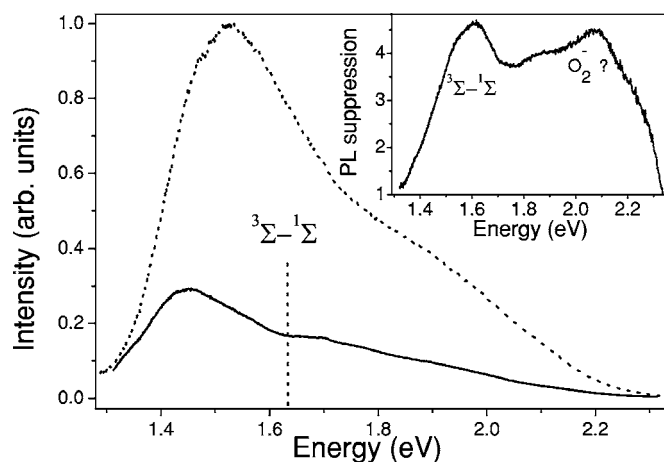


FIG. 8. PL spectra of *PSi* powder immersed in degassed water (dotted line) and in oxygen-saturated water (solid line). Inset: spectral dependence of the PL suppression level measured for *PSi* powder immersed in oxygen-saturated water. $T=300$ K, $E_{ex}=2.54$ eV. Energy of the $^3\Sigma-^1\Sigma$ transition of O_2 is indicated by a dotted line.

gaseous oxygen ambient (see Fig. 9). The exciton lifetimes for silicon nanocrystals immersed in degassed water are identical to those measured in vacuum. Oxygen dissolved in water causes its significant shortening over all spectral range investigated. The spectral dependence of the energy transfer time is very similar to that observed for gaseous oxygen ambient (see inset of Fig. 9). A slightly longer energy transfer time of $30 \mu s$ is still shorter than the exciton lifetime what is in good agreement with the observed small difference in the PL suppression levels.

IV. CONCLUSIONS

Time-resolved PL spectroscopy allowed us to analyze the energy transfer processes in the strongly coupled exciton- O_2

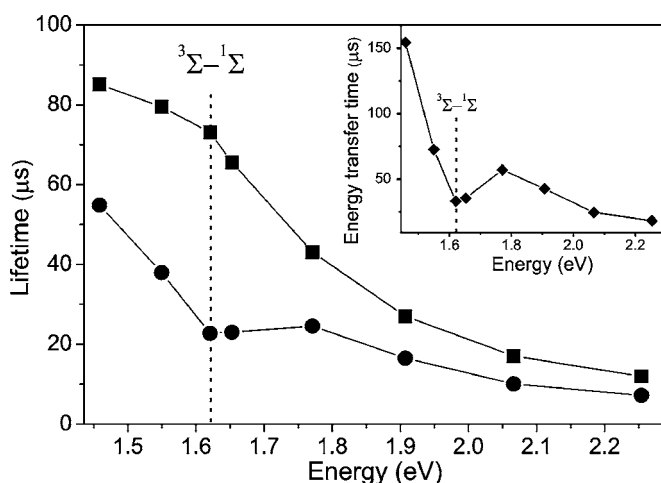


FIG. 9. Spectral dependencies of the PL lifetime measured in degassed water (squares) and in oxygen-saturated water (circles). Inset: spectral dependence of the energy transfer time in oxygen-saturated water. $T=300$ K, $E_{ex}=2.33$ eV. Energy of the $^3\Sigma-^1\Sigma$ transition of O_2 is indicated by a dotted line.

system. We demonstrated that the energy transfer time is the shortest for excitons having exactly the energy of the $^3\Sigma-^1\Sigma$ transition. At the lower PL energy side of the $^3\Sigma-^1\Sigma$ transition energy, a spectral signature corresponding to momentum-conserving phonons and, at the higher energy side, those due to the emission of energy-conserving phonons are observed. The energy transfer time becomes about 40% longer due to the involvement of one transversal optical phonon for energy conservation. This suggests that an accurate tuning of the band-gap energy is required for Si nanocrystal assemblies to realize the highest energy transfer efficiency. The energy transfer time to oxygen dimers is found to be much shorter than that to O_2 followed by excitation of the $^1\Delta$ state and of the same order for the $^3\Sigma-^1\Sigma$ transition.

The spectral signatures observed in inhomogeneously broadened PL bands of *PSi* are similar to spectral holes in the hole-burning spectroscopy, and they provide valuable information about electronic structures of size-selected and, therefore, energy-selected Si nanocrystals. Presented results clearly demonstrate that Si nanocrystals with a band-gap energy of 1.96 eV strongly hold the indirect band-gap nature of bulk Si crystals and $TO(\Delta)$ phonon-assisted recombination is

still the dominant recombination path. Furthermore, involvement of characteristic momentum- and energy-conserving phonons known for bulk Si evidences that excitons are localized in Si nanocrystal cores.

At room temperature, despite shorter exciton lifetime, excitons confined in Si nanocrystals can also efficiently transfer their energies to oxygen molecules either in gaseous form or dissolved in water. The high efficiency of the energy transfer at room temperature, crucial for biological and medical applications of Si nanocrystals, is governed by the long lifetime of confined indirect excitons. From the point of view of practical applications, specifically in medicine, Si nanocrystals in colloidal form should act in a similar way as conventional dye molecules.

ACKNOWLEDGMENTS

This work is supported by Industrial Technology Research Grant Program from New Energy and Industrial Technology Development Organization (NEDO) Japan and by Commission of the European Communities, 6th Framework Program (STRP 013875).

- ¹A. G. Cullis, L. T. Canham, and P. D. J. Calcott, *J. Appl. Phys.* **82**, 909 (1997).
- ²L. Pavesi, C. Mazzoleni, L. Dal Negro, G. Franzo, and F. Priolo, *Nature (London)* **408**, 440 (2000).
- ³L. Khriachtchev, M. Räsänen, S. Novikov, and J. Sinkkonen, *Appl. Phys. Lett.* **79**, 1249 (2001).
- ⁴L. Dal Negro, M. Cazzanelli, L. Pavesi, S. Ossicini, D. Pacifici, G. Franzo, and F. Priolo, *Appl. Phys. Lett.* **82**, 4636 (2003).
- ⁵S. Takeoka, M. Fujii, and S. Hayashi, *Phys. Rev. B* **62**, 16820 (2000).
- ⁶L. Brus, in *Light Emission in Silicon*, edited by D. J. Lockwood (Academic Press, New York, 1996).
- ⁷F. Huisken, G. Ledoux, O. Guillois, and C. Reynaud, *Adv. Mater.* **14**, 1861 (2002).
- ⁸D. Kovalev, E. Gross, N. Künzner, F. Koch, V. Yu. Timoshenko, and M. Fujii, *Phys. Rev. Lett.* **89**, 137401 (2002).
- ⁹E. Gross, D. Kovalev, N. Künzner, J. Diener, F. Koch, V. Yu. Timoshenko, and M. Fujii, *Phys. Rev. B* **68**, 115405 (2003).
- ¹⁰M. Fujii, S. Minobe, M. Usui, S. Hayashi, E. Gross, J. Diener, and D. Kovalev, *Phys. Rev. B* **70**, 085311 (2004).
- ¹¹N. J. Turro, *Modern Molecular Photochemistry* (University Science Books, Sausalito, CA, 1991).
- ¹²L. Packer and H. Sies, *Singlet Oxygen, UV-A, and Ozone* (Academic Press, London, 2000).
- ¹³C. Schweitzer and R. Schmidt, *Chem. Rev. (Washington, D.C.)* **103**, 1685 (2003).
- ¹⁴D. B. Min, and J. M. Boff, *Comprehensive Reviews in Food Science and Food Safety* **1**, 58 (2002).
- ¹⁵J. G. Moser, *Photodynamic Tumor Therapy: 2nd and 3rd Generation Photosensitizers* (G and B Science Pub., Amsterdam 1998).
- ¹⁶D. Kovalev, H. Heckler, G. Polisski, and F. Koch, *Phys. Status Solidi B* **215**, 871 (1999).
- ¹⁷L. T. Canham, *Appl. Phys. Lett.* **57**, 1046 (1990).
- ¹⁸P. D. J. Calcott, K. J. Nash, L. T. Canham, M. J. Kane, and D. Brumhead, *J. Phys.: Condens. Matter* **5**, L91 (1993).
- ¹⁹A. G. Cullis, L. T. Canham, and P. D. J. Calcott, *J. Appl. Phys.* **82**, 909 (1997).
- ²⁰D. Kovalev, B. Averboukh, M. Ben-Chorin, F. Koch, Al. L. Efros, and M. Rosen, *Phys. Rev. Lett.* **77**, 2089 (1996); D. Kovalev, H. Heckler, B. Averboukh, M. Ben-Chorin, M. Schwartzkopff, and F. Koch, *Phys. Rev. B* **57**, 3741 (1998).
- ²¹M. Fujii, Y. Yamaguchi, Y. Takase, K. Ninomiya, and S. Hayashi, *Appl. Phys. Lett.* **85**, 1158 (2004).
- ²²E. A. Konstantinova, L. A. Osminkina, K. S. Sharov, E. V. Kurepina, P. K. Kashkarov, and V. Y. Timoshenko, *JETP* **99**, 741 (2004).
- ²³G. Davies, *Phys. Rep.* **176**, 83 (1989).
- ²⁴D. Kovalev, H. Heckler, M. Ben-Chorin, G. Polisski, M. Schwartzkopff, and F. Koch, *Phys. Rev. Lett.* **81**, 2803 (1998).
- ²⁵A. U. Khan, and M. Kasha, *J. Am. Chem. Soc.*, **92**, 3293 (1970).
- ²⁶D. Kovalev, B. Averboukh, M. Ben-Chorin, F. Koch, Al. L. Efros, and M. Rosen, *Phys. Rev. Lett.* **77**, 2089 (1996).